XXXth IAU General Assembly, August 2018
Chanda Jog & Danail Obreschkow, ed.
DOI: 10.5281/zenodo.1481572

Angular Momentum-Mass Law for Discs in the Nearby Universe

Lorenzo Posti
Kapteyn Astronomical Institute, University of Groningen, P.O. Box 800, 9700 AV Groningen, the Netherlands
email: `posti@astro.rug.nl`

Abstract. The relation between galaxy mass and specific angular momentum is a fundamental scaling law of galaxy structure, however accurate observational determinations are made difficult by the fact that most of the specific angular momentum of a typical galaxy resides in its outer regions. I measure the stellar specific angular momenta for 154 disc galaxies at $z = 0$ (with $7 \lesssim \log M_\star/M_\odot \lesssim 11.5$) using HI rotation curves to trace stellar rotation typically beyond 5 disc scale-lengths. An accurate measurement of $j_\star$ can be derived for $\sim 60\%$ of the sample, while only lower limits can be inferred for the remaining $\sim 40\%$. I derive fits to the specific stellar angular momentum-stellar mass scaling law ($j_\star - M_\star$) both considering only 92 accurate measurements and taking into account also for 62 lower limits: I find no significant differences in these two cases. I also show how the intrinsic scatter of the $j_\star - M_\star$ relation varies as a function of the mass-to-light ratio adopted to determine the stellar masses.

Keywords. galaxies: kinematics and dynamics, galaxies: spiral, galaxies: structure

1. Introduction

Many important insights in galaxy formation and evolution can be gained by studying scaling relations of galaxy properties. Mass and specific angular momentum (i.e. angular momentum normalized by mass) are two of the most fundamental structural properties of galaxies, which are independent and subject to physical conservation laws. The scaling relation that they define, first analyzed by Fall (1983, thus hereafter *the Fall relation*), has the unique power of constraining an important aspect of galaxy formation, namely the link between the spins of galaxies and of dark matter halos (Romanowsky & Fall 2012; Shi et al. 2017; Posti et al. 2018a). However, understanding this scaling law, and hence how galaxies acquire their spin, is complicated by the fact that typically most of the angular momentum resides in the outer parts of the system, where observations are significantly more difficult. For instance, an exponential disc with a flat rotation curve has $\gtrsim 50\%$ of its specific angular momentum outside two disc scale-lengths, where spectroscopic observations are challenging. Thus, tracers of the rotation velocity of galaxies that extend further away from the centre are needed to accurately characterize the Fall relation.

Here I focus on the *stellar* Fall relation: the $j_\star - M_\star$ relation, where $M_\star$ and $j_\star$ are the stellar mass and stellar specific angular momentum respectively. Together with a stellar-to-halo mass relation, this can be used to empirically estimate the stellar-to-halo specific angular momentum relation, which is the main ingredient that sets galaxy sizes and morphologies in a galaxy formation model (e.g., Posti et al. 2018a).

2. The $j_\star - M_\star$ relation for nearby disc galaxies

I use the sample of 175 nearby disc galaxies collected by Lelli et al. (2016, hereafter SPARC) for which both accurate HI rotation curves and Spitzer photometry at 3.6μm are

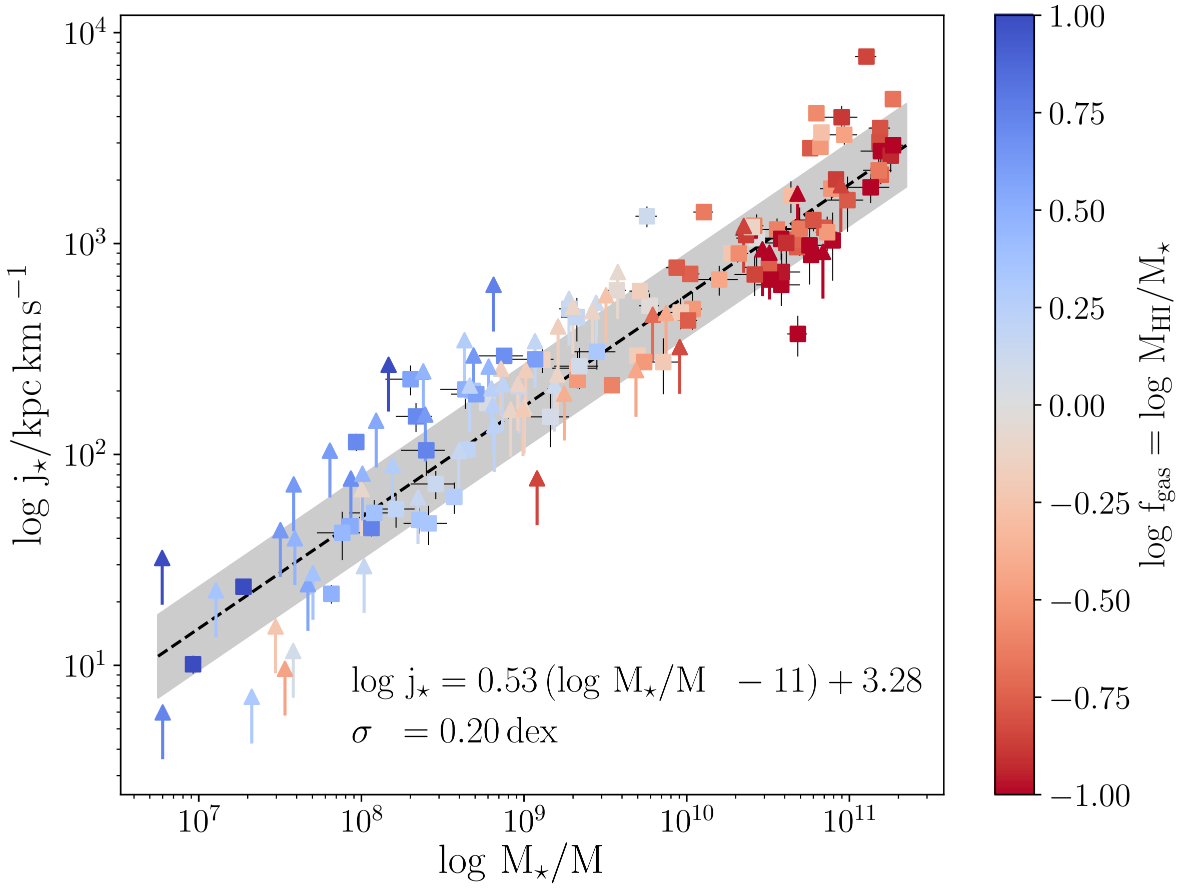

Figure 1. Stellar specific angular momentum-stellar mass relation (Fall relation) for 154 galaxies in the nearby Universe from the SPARC sample. Squares (with 1-σ uncertainties) are the accurate measurements for 92 galaxies with a converged $j_\star(<R)$ profile, while upwards arrows are lower limits for the 62 ones with non-converging profiles. The points are colour-coded by the logarithm of the gas fraction. The best-fit power-law relation, accounting also for the lower limits, is shown with a black dashed line (with the grey band representing the 1-σ intrinsic scatter).

available. Near-infrared photometry is used to trace the stellar mass surface density $\Sigma_\star$ within the galaxy, with the total stellar mass $M_\star$ being computed using constant mass-to-light ratios for the disc and the bulge component respectively $(\Upsilon_{\rm d}^{[3.6]}, \Upsilon_{\rm b}^{[3.6]}) = (0.5, 0.7)$; while the neutral hydrogen rotation curves are used to trace the stellar rotation velocity $V_\star$, after correcting for asymmetric drift (see Posti et al. 2018b, for details). I compute stellar specific angular momentum profiles as

$$j_\star(<R) = \frac{\int_0^R \mathrm{d}R'\, R'^2\, \Sigma_\star(R')\, V_\star(R')}{\int_0^R \mathrm{d}R'\, R'\, \Sigma_\star(R')} \tag{2.1}$$

and I define $j_\star$ for each galaxy as the last measured point of the $j_\star(<R)$ profile. A selection of galaxies observed at inclinations larger than 30° leaves us with 154 galaxies: this is needed since for nearly face-on systems the HI rotation curves are too uncertain. Out of these 154 objects, 92 have converged $j_\star(<R)$ profiles (i.e. they satisfy criteria (2) in Posti et al. 2018b): for these galaxies the total stellar specific angular momentum is accurately measured (better than 10%). The $j_\star(<R)$ profiles of the other 62 systems are instead still rising to the outermost measured point, thus the estimated $j_\star$ can only be considered as a lower limit of the actual stellar specific angular momentum. In Fig. 1 I

plot the accurately measured $j_\star$ as a function of $M_\star$ for the 92 galaxies as squares (with 1-σ errorbars), while upwards arrows represent the lower limits on $j_\star$ for the other 62 galaxies in the SPARC sample. The distribution of lower limits is completely compatible with that of the accurate measurements, with galaxies with more steeply rising $j_\star(< R)$ in the outermost measured points being found at lower specific angular momenta with respect to galaxies with similar stellar mass.

In Posti et al. (2018b) we presented best-fitting power-law scaling relations when only considering the 92 galaxies for which accurate $j_\star$ measurements could be obtained. Here I take into account also the other 62 lower limits and fit the $j_\star - M_\star$ relation similarly to Posti et al. (2018b). I find a perfectly compatible best-fitting model with slope $\alpha = 0.53 \pm 0.3$, normalization $\beta = 3.28 \pm 0.05$ and a slightly larger orthogonal intrinsic scatter of $\sigma_\perp = 0.2 \pm 0.02$ dex. I overplot this best-fit to the measurements and lower limits in Fig. 1.

Bulge fraction, which can be considered a proxy for galaxy morphology, is known to play an important role in the $j_\star - M_\star$ diagram, with galaxies with increasing bulge fractions having smaller $j_\star$ for a fixed $M_\star$ (see e.g. Romanowsky & Fall 2012). If for a fixed mass angular momentum traces bulge fraction, then it follows that the $j_\star - M_\star$ law for galaxies of a specific bulge fraction (i.e. of a fixed morphological type) should have the smallest intrinsic scatter. Moreover, in Posti et al. (2018b) we showed that the relation obtained only considering the discs of the 92 spiral galaxies with accurate $j_\star$ measurements has a smaller $\sigma_\perp$ with respect to the relation derived when including also their bulges. Here I systematically assess how does the orthogonal intrinsic scatter $\sigma_\perp$ of the $j_\star - M_\star$ relation varies when changing the mass-to-light ratios of the disc ($\Upsilon_{\rm d}^{[3.6]}$) and the bulge component ($\Upsilon_{\rm b}^{[3.6]}$). In Fig. 2 I show $\sigma_\perp$ as a function of $\Upsilon_{\rm d}^{[3.6]}$ and $\Upsilon_{\rm b}^{[3.6]}$, where these two vary in the range $[0.1, 1]$. Reasonable assumptions are typically those where $\Upsilon_{\rm b}^{[3.6]} \geqslant \Upsilon_{\rm d}^{[3.6]}$: for instance, stellar population models suggest $\Upsilon_{\rm b}^{[3.6]} = 1.4\Upsilon_{\rm d}^{[3.6]}$ (Schombert & McGaugh 2014). Fig. 2 shows that for reasonable choices of the mass-to-light ratios the intrinsic scatter cannot be smaller than $\sigma_\perp \sim 0.17$ dex. However, for any given $\Upsilon_{\rm d}^{[3.6]}$ I find the smallest $\sigma_\perp$ for $\Upsilon_{\rm b}^{[3.6]} \sim 0$, confirming our previous result that the $j_\star - M_\star$ relation for only the discs of spiral galaxies has the smallest intrinsic scatter (Posti et al. 2018b).

3. Conclusions

The Fall relation has become a fundamental test-bed for analytic, semi-analytic and numerical galaxy formation models. The straightness and tightness that it exhibits, over ~ 5 orders of magnitude in stellar mass for disc galaxies in the nearby Universe, demand to be reproduced by any model that aspires to be deemed as successful. While the samples accurately analyzed up to now are representative of the galaxy population, they are not complete or volume-limited. In the future we will need to measure extended angular momentum profiles for a much larger sample, and possibly complete and/or volume-limited, of both late-type and early-type galaxies. This can be done with surveys using the next generation of Integral Field Spectrographs in the optical domain and with new upcoming H I blind surveys of spatially resolved galaxies in the radio domain. This will also be helpful for modellers to constrain their formation theories without worrying about selection effects.

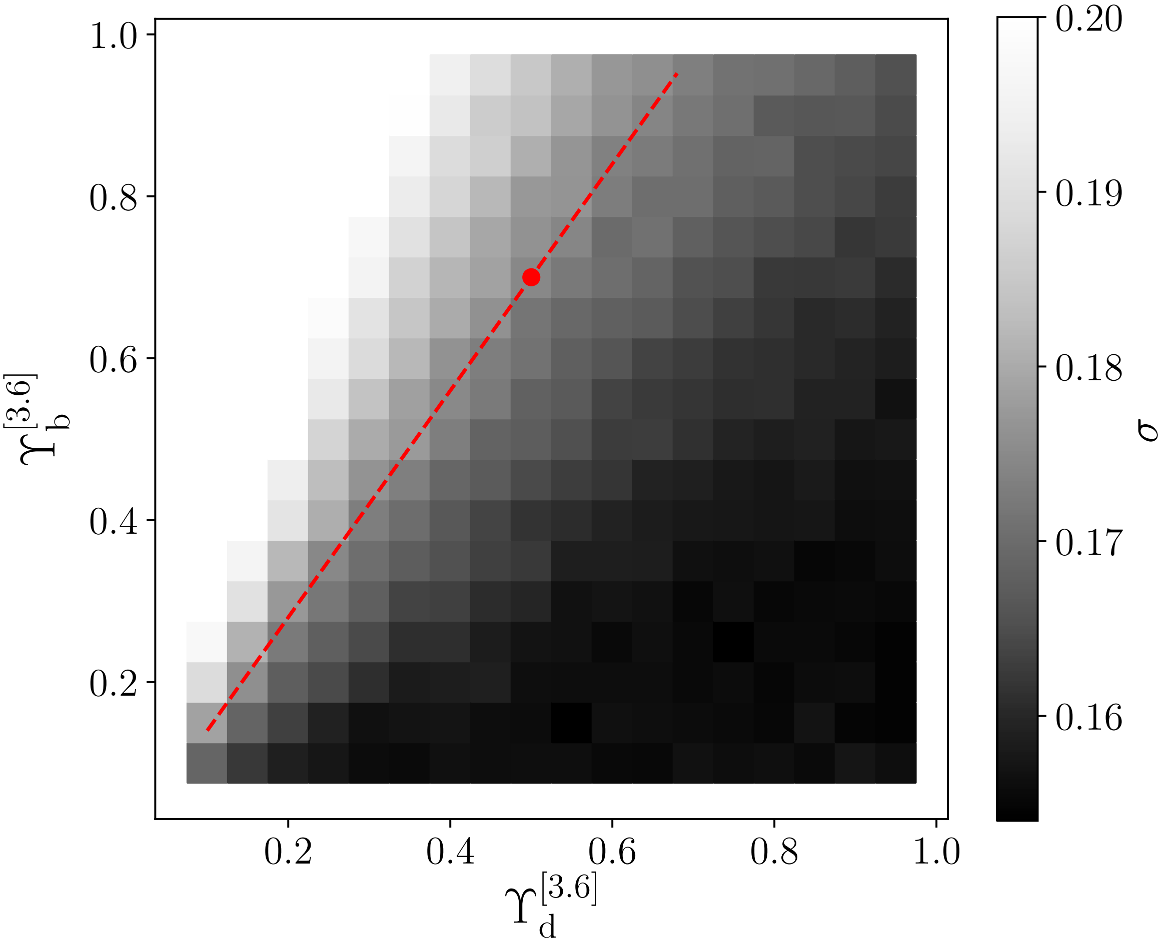

Figure 2. Orthogonal intrinsic scatter of the Fall relation, as in Fig. 1, as a function of the disc and bulge mass-to-light ratios. The red dashed line is $\Upsilon_{\rm b}^{[3.6]} = 1.4\Upsilon_{\rm d}^{[3.6]}$, the locus of values suggested by stellar population models (Schombert & McGaugh 2014), while the red dot is the fiducial value used in Fig. 1.

References

Fall S. M., 1983, IAUS, 100, 391
Lelli F., McGaugh S. S., Schombert J. M., 2016, AJ, 152, 157
Romanowsky A. J., Fall S. M., 2012, ApJS, 203, 17
Posti L., Pezzulli G., Fraternali F., Di Teodoro E. M., 2018a, MNRAS, 475, 232
Posti L., Fraternali F., Di Teodoro E. M., Pezzulli G., 2018b, A&A, 612, L6
Schombert J., McGaugh S., 2014, PASA, 31, e036
Shi J., Lapi A., Mancuso C., Wang H., Danese L., 2017, ApJ, 843, 105